



## OPEN ACCESS

## EDITED BY

Xinli Zhou,  
Southwest University of Science and  
Technology, China

## REVIEWED BY

Haifeng Liu,  
Chonnam National University,  
Republic of Korea  
Xiaojun Nie,  
Northwest A&F University, China  
Xiaodong Wang,  
Hebei Agricultural University, China  
Huan Luo,  
Chungnam National University,  
Republic of Korea

## \*CORRESPONDENCE

Wang Chen

✉ chenwangchw@163.com

Zhengwu Fang

✉ fangzhengwu88@163.com

Wenli Wang

✉ wliw@163.com

†These authors have contributed  
equally to this work

RECEIVED 23 April 2023

ACCEPTED 09 June 2023

PUBLISHED 05 July 2023

## CITATION

Feng Y, Tang M, Xiang J, Liu P, Wang Y,  
Chen W, Fang Z and Wang W (2023)  
Genome-wide characterization of L-  
aspartate oxidase genes in wheat and  
their potential roles in the responses to  
wheat disease and abiotic stresses.  
*Front. Plant Sci.* 14:1210632.  
doi: 10.3389/fpls.2023.1210632

## COPYRIGHT

© 2023 Feng, Tang, Xiang, Liu, Wang, Chen,  
Fang and Wang. This is an open-access  
article distributed under the terms of the  
[Creative Commons Attribution License  
\(CC BY\)](https://creativecommons.org/licenses/by/4.0/). The use, distribution or  
reproduction in other forums is permitted,  
provided the original author(s) and the  
copyright owner(s) are credited and that  
the original publication in this journal is  
cited, in accordance with accepted  
academic practice. No use, distribution or  
reproduction is permitted which does not  
comply with these terms.

# Genome-wide characterization of L-aspartate oxidase genes in wheat and their potential roles in the responses to wheat disease and abiotic stresses

Yanqun Feng<sup>1†</sup>, Mingshuang Tang<sup>2†</sup>, Junhui Xiang<sup>1</sup>, Pingu Liu<sup>1</sup>,  
Youning Wang<sup>3</sup>, Wang Chen<sup>1\*</sup>, Zhengwu Fang<sup>1\*</sup>  
and Wenli Wang<sup>4\*</sup>

<sup>1</sup>Ministry of Agriculture and Rural Affairs (MARA) Key Laboratory of Sustainable Crop Production in the Middle Reaches of the Yangtze River (Co-Construction by Ministry and Province)/Engineering Research Center of Ecology and Agricultural Use of Wetland, Ministry of Education, Hubei Collaborative Innovation Center for Grain Industry, College of Agriculture, Yangtze University, Jingzhou, China, <sup>2</sup>Nanchong Academy of Agriculture Sciences, Nanchong, Sichuan, China, <sup>3</sup>Hubei Key Laboratory of Quality Control of Characteristic Fruits and Vegetables, Hubei Engineering University, Xiaogan, Hubei, China, <sup>4</sup>College of Plant Protection, Northwest A&F University, Yangling, Shaanxi, China

L-aspartate oxidase (AO) is the first enzyme in NAD<sup>+</sup> biosynthesis and is widely distributed in plants, animals, and microorganisms. Recently, AO family members have been reported in several plants, including *Arabidopsis thaliana* and *Zea mays*. Research on AO in these plants has revealed that AO plays important roles in plant growth, development, and biotic stresses; however, the nature and functions of AO proteins in wheat are still unclear. In this study, nine AO genes were identified in the wheat genome *via* sequence alignment and conserved protein domain analysis. These nine wheat AO genes (*TaAOs*) were distributed on chromosomes 2, 5, and 6 of sub-genomes A, B, and D. Analysis of the phylogenetic relationships, conserved motifs, and gene structure showed that the nine *TaAOs* were clustered into three groups, and the *TaAOs* in each group had similar conserved motifs and gene structure. Meanwhile, the subcellular localization analysis of transient expression mediated by *Agrobacterium tumefaciens* indicated that *TaAO3-6D* was localized to chloroplasts. Prediction of cis-elements indicated that a large number of cis-elements involved in responses to ABA, SA, and antioxidants/electrophiles, as well as photoregulatory responses, were found in *TaAO* promoters, which suggests that the expression of *TaAOs* may be regulated by these factors. Finally, transcriptome and real-time PCR analysis showed that the expression of *TaAOs* belonging to Group III was strongly induced in wheat infected by

*F. graminearum* during anthesis, while the expression of TaAOs belonging to Group I was heavily suppressed. Additionally, the inducible expression of TaAOs belonging to Group III during anthesis in wheat spikelets infected by *F. graminearum* was repressed by ABA. Finally, expression of almost all TaAOs was induced by exposure to cold treatment. These results indicate that TaAOs may participate in the response of wheat to *F. graminearum* infection and cold stress, and ABA may play a negative role in this process. This study lays a foundation for further investigation of TaAO genes and provides novel insights into their biological functions.

#### KEYWORDS

TaAO, gene structure, abiotic stresses, gene expression, quantitative PCR, biological functions

## 1 Introduction

L-aspartate oxidase (AO), a kind of flavin oxidase, converts aspartate to iminoaspartic acid using either molecular oxygen or fumarate as electron acceptors. It plays an indispensable role in the biosynthesis of nicotinamide adenine dinucleotide (NAD<sup>+</sup>) (Mattevi et al., 1999). NAD<sup>+</sup> biosynthesis consists of five steps, of which the first is oxidation of L-aspartate into iminoaspartate catalyzed by L-aspartate oxidase (Kato et al., 2006). NAD<sup>+</sup> is an important component of the respiratory chain, so it plays an important role in biological energy metabolism. It additionally participates in reduction-oxidation reactions, DNA repair, ADP-ribosylation, and a series of metabolic processes (Gakiere et al., 2018). L-aspartate oxidase, as the enzyme of the first reaction in *de novo* synthesis of NAD<sup>+</sup>, is also thought to play an important role in the energy metabolism system and other metabolic pathways in organisms. Therefore, AO has been researched extensively over the years.

AO was initially reported in *Escherichia coli*, where the B protein of quinolinic synthase was identified as a L-aspartate oxidase (Nasu et al., 1982). Later, two conserved domains, the FAD binding domain and Succ\_DH\_flav\_C, were found in AO proteins (Mattevi et al., 1999). Subsequently, AO was identified in *Pyrococcus shorikishii* OT-3 (Sakuraba et al., 2002), *Sulfolobus tokodaii* (Sakuraba et al., 2008), *Bacillus subtilis* (Marinoni et al., 2008), and *Pseudomonas putida* (Leese et al., 2013). Since then, the physiological and biochemical properties of AO have been extensively investigated in bacteria (Mortarino et al., 1996; Bifulco et al., 2013; Armenia et al., 2017; Chow et al., 2017). AO has the following two features: (a) *in vitro*, it is able to use different electron acceptors, such as oxygen, fumarate, cytochrome c, and quinones, suggesting that it is involved in NAD biosynthesis in anaerobic as well as aerobic conditions (Tedeschi et al., 1996); and (b) the primary and tertiary structures are not similar to those of other flavo-oxidases, but rather are similar to those of the flavoprotein subunit of the succinate dehydrogenase/fumarate reductase class of enzymes. AO can reduce fumarate and oxidize L-aspartate, but cannot oxidize succinate (Bacchella et al., 1999; Tedeschi et al.,

2010). It has been reported that *Shigella*, a nicotinic acid auxotroph, is unable to synthesize NAD *via* the *de novo* pathway due to AO gene mutations. When AO function is restored in *Shigella*, sustained loss of virulence and inability to invade host cells are observed, which points toward AO as a locus of antivirulence (Prunier et al., 2007).

Compared with microorganisms, little is still known about AO in plants. Up to this point, AO proteins have been reported only in maize and *A. thaliana*. In maize, a gene *GRMZM2G139689* has been reported to encode AO protein. At the mononuclear stage of microspore development, the expression level of this gene was found to be greatly downregulated in male sterile line C48-2 compared with maintainer line 48-2 (Dong, 2019). This suggests that AO protein may be involved in pollen abortion in maize. In *A. thaliana*, *At5g14760* has been identified as an AO (Macho et al., 2012). Overexpression of *AtAO* increases NAD<sup>+</sup> content, and loss of *AtAO* activity results in a decrease in NAD<sup>+</sup> levels (Hao et al., 2018). It is worth noting that the expression of AOs is upregulated in *A. thaliana* leaves infected by avirulent *Pseudomonas syringae* pv. *tomato* strain (Petriacq et al., 2012). Furthermore, research with an AO *A. thaliana* mutant has shown that AO is required for reactive oxygen species (ROS) bursts triggered by pathogen-associated molecular patterns and for stomatal immunity (Macho et al., 2012). These studies indicate that AO genes play important roles in regulating plant development and response to biotic stresses.

Wheat is one of the top three crops worldwide (Guo et al., 2018). Almost 60% of the wheat produced globally is consumed as food (Sobolewska et al., 2020), and global demand for wheat is expected to grow by approximately 70% over the next 30 years with growing populations, rising income levels, and increasing household consumption (Abedi and Mojiri, 2020). Wheat often suffers from exposure to biotic and abiotic stresses during growth; it is unclear whether wheat AO participates in the plant's response to biotic/abiotic stresses, and the molecular characteristics of wheat AO are also unclear. In this study, TaAO genes were identified *via* sequence alignment and protein domain analysis, and the gene structure, phylogenetic relationships, and chromosome distribution of TaAO family genes were subsequently analyzed systematically

using bioinformatics methods. Finally, the expression patterns of *TaAO* family genes were quantified *via* transcriptome analysis and qRT-PCR. This study lays a foundation for further analysis of *AO* genes in wheat.

## 2 Materials and methods

### 2.1 Genome-wide identification of *AO* genes in *T. aestivum*, *Ae. tauschii*, *T. urartu*, and *T. dicoccoides*

Genome data for *T. aestivum* (IWGSCv2.1), *Ae. tauschii* (v4.0.43), *T. urartu* (v1.43), and *T. dicoccum* (v1.0.43) were downloaded from Ensembl Plants database (<http://plants.ensembl.index.html>). Hidden Markov models (HMMs) for the FAD binding domain (PF00890.27) and the Succ\_DH\_flav\_C domain (PF02910.23), obtained from the Pfam database (<http://pfam.xfam>), were used as queries to identify wheat AOs using HMMER3.0 (<http://hmmmer.download.html>) with hit sequences specified as those with an e-value below  $1e^{-5}$ . Three *Arabidopsis* AOs (AtAOs), three maize AOs (ZmAOs), and two rice AOs (OsAOs), where the identification method was similar to that of *TaAOs*, were retrieved from genome databases for *Arabidopsis* (<http://www.arabidopsis.index.jsp>), maize (<https://www.maizegdb.org>), and rice (<http://rice.plantbiology.msu.edu>), respectively (Table S1). These *AO* proteins were used as queries to search for *AO* proteins in the genomes of *T. aestivum*, *Ae. tauschii*, *T. urartu*, and *T. dicoccoides* *via* BLASTp. Hit sequences with an e-value below  $1e^{-5}$  were retained. The wheat *AO* candidates obtained using the above two methods were combined, and the non-redundant proteins were further analyzed using Pfam (v31.05) (<http://pfam.sanger.ac.uk/search>) and SMART (<http://smart.embl-heidelberg.de/>) (Letunic and Bork, 2018). Only these proteins that contained both the FAD binding domain and the Succ\_DH\_flav\_C domain were considered to be wheat AOs. The *AO* genes were named according to their distribution on the chromosomes.

### 2.2 Characteristics of *TaAO* proteins

The protein sequence length, isoelectric point (pI), molecular weight (MW), instability index, and grand average of hydropathicity (GRAVY) of *TaAOs* were predicted using the ExPASy online tool (<https://www.expasy.org/>) (Gasteiger et al., 2003). Subcellular localization of *TaAOs* was predicted using the WoLF PSORT online tool (<https://wolfpsort.hgc.jp/>) (Chou and Shen, 2010).

### 2.3 Phylogenetic analysis of *TaAOs*

The sequences of *AO* proteins from *A. thaliana*, rice, maize, *T. aestivum*, *Ae. tauschii*, *T. urartu*, and *T. dicoccoides* were aligned using the ClustalW2 software package (Thompson et al., 1994). A neighbor-joining (NJ) phylogenetic tree was constructed using the

MEGA X software package (Mega Limited, Auckland, New Zealand) (Kumar et al., 2018) with 1000 bootstrap repetitions. Finally, the tree was modified using the Interactive Tree of Life tool (iTOL, v6, <http://itol.embl.de>) (Letunic and Bork, 2021).

### 2.4 Genomic organization of *TaAOs* in wheat

Information on the position of *TaAOs* in wheat chromosomes was extracted from annotated information on the wheat genome. The physical map was drawn using the MapInspect software package. Information on the exon–intron structure of *TaAO* genes was visualized using the TBtools software package (Chen et al., 2020). Conserved motifs of *TaAOs* were identified using the MEME suite, with the following parameter settings: number of motifs, up to 15; width range, from 6 to 50 amino acids. The outputs on the motif structures of *TaAO* proteins were displayed using TBtools. Gene duplication events were analyzed according to the method described by Panchy et al. (2016) and illustrated using the Circos package in TBtools. For further examination of the footprints of selection during the processes of domestication (wild emmer and *Ae. tauschii* versus landraces) and improvement (landraces versus varieties), we overlapped the identified *AO* genes with the sweep region identified by Cheng et al. (2019) to check whether they were selected. The *Ka* and *Ks* values and the *Ka/Ks* ratio were calculated using TBtools. A *Ka/Ks* value of 1 indicates a neutral selection effect; a *Ka/Ks* value >1 indicates positive selection for evolutionary acceleration; and *Ka/Ks* <1 indicates purifying selection under function constraints.

### 2.5 RNA isolation and cDNA first-strand synthesis

Total RNA was extracted using TRIzol reagent (Invitrogen, USA) according to the manufacturer's instructions. Subsequently, 1  $\mu$ g RNA was used for cDNA first-strand synthesis using a PrimeScript RT reagent kit with gDNA Eraser (Takara, China) according to the manufacturer's instruction.

### 2.6 Subcellular localization analysis of *TaAO3-6D* protein

Subcellular localization analysis of a *TaAO* protein was performed using an *Agrobacterium tumefaciens* mediated transient expression system in leaves of *Nicotiana benthamiana*. First, the coding sequence of a *TaAO*, *TaAO3-6D*, was amplified (the primers are listed in Table S2) and cloned into a GFP fusion protein expression vector pCAMBIA1300-GFP. Next, the recombinant vector was transformed into an *Agrobacterium tumefaciens* GV3101 strain. Positive clones were cultured and injected into the leaves of 5- to 6-week-old *Nicotiana benthamiana*. These were observed using a fluorescence microscope (Olympus FV3000, Tokyo, Japan) 48 h after injection.

## 2.7 Cis-acting element and protein interaction network analyses of TaAOs

The 1.5 kb sequence upstream of the start codon of each of the *TaAO* genes was obtained, and these sequences were used for the prediction of cis-acting elements *via* the PlantCARE website (<http://bioinformatics.psb.ugent.be/webto-ols/plantcare/html/>). The cis-acting elements were arranged and displayed using the R software package “pheatmap” (Rombauts et al., 1999). To study the protein–protein interactions (PPIs) between TaAOs and other proteins, a protein network was generated using the STRING v11.5 webserver (<https://cn.string-db.org/>).

## 2.8 Expression profiling of *TaAO* genes *via* transcriptome analysis

Transcriptome data on sequences involved in wheat growth and wheat responses to biotic stresses (*Fusarium graminearum*, stripe rust, and wheat powdery mildew) and abiotic stresses (phosphorous starvation, cold, heat, and drought) were downloaded from the NCBI database (Table S3) and mapped to the wheat reference genome *via* Hisat2 (Fang et al., 2020). The expression levels of *TaAOs* were calculated using Cufflinks (Trapnell et al., 2012). All transcript values were standardized by  $\log_2$  (TPM + 1) transformation, and the expression profiles of *TaAOs* were generated using the R package “pheatmap”.

## 2.9 Growth and stress treatments of wheat seedlings

Jingshuang 16, a wheat cultivar moderately susceptible to powdery mildew and rust (Ren et al., 2015), was used in this study. The wheat seeds were disinfected with 1% hydrogen peroxide; subsequently, after washing with distilled water, the seeds were kept at 25°C for 2 days for germination. The seedlings were cultured in quarter-strength Hoagland nutrient solution for 3 days, and then transferred to one-half Hoagland nutrient solution (pH=6.0) (Bishop and Bugbee, 1998). To examine the differential expression of *TaAOs* in response to drought and abscisic acid (ABA) treatment, seedlings were cultured in a greenhouse at 25/20°C under a 16 h light/8 h dark cycle. The seedlings were treated with 20% PEG6000, once at the heart stage and once at the leaf stage. Wheat leaves were sampled at 0, 2, 12, 24, 36, and 48 h after treatment. For the ABA treatment, ABA was added to one-half strength Hoagland nutrient solution at a final concentration of 100  $\mu$ M. After 0, 2, 6, 12, 24, and 48 h of treatment, leaves were harvested for further research. Finally, for the stripe rust infection treatment, seedlings were cultured in a plant growth chamber under a 16 h light/8 h dark cycle at 16°C. Wheat leaves were inoculated with fresh uredospores of stripe rust CYR32 using the smearing method and kept in dark, moist conditions for 24 hours to promote infection (Santra et al., 2008). Leaves were collected at 0, 6, 12, 24, and 48 h. All samples were immediately frozen in liquid nitrogen and stored at -80°C for future use.

## 2.10 qRT-PCR analysis

Real-time PCR reaction systems were used to carry out reaction schemes following the manufacturer’s instruction (Vazyme, China). Gene-specific primers (Table S4) were designed using the Primer 5.0 software package. The ADP-ribosylation factor *Ta2291* was used as the internal reference gene for qRT-PCR analysis. Each experiment was carried out with three biological replicates, and three technical repeats were performed for each replicate.

## 3 Results

### 3.1 Identification and classification of AO genes in wheat

Ten AO candidates were obtained from the wheat genome *via* HMM search. Meanwhile, the same ten AO candidates were retrieved from the wheat genome *via* BLASTp. Of these, one gene without the Succ\_DH\_flav\_C domain was excluded, and the remaining nine candidate genes containing both of the FAD binding domain and the Succ\_DH\_flav\_C domain were identified as *TaAOs* (Table 1; Table S5). Using the same procedure, four, three, and six AOs were identified for *T. urartu*, *Ae. Tauschii*, and *T. dicoccoides*, respectively (Table S4). The locations of AO genes on the wheat chromosomes were determined and analyzed for genomic homology; this analysis indicated that nine *TaAO* genes were distributed evenly on chromosomes 2, 5, and 6 of sub-genomes A, B, and D, while no tandem duplication or segmental duplication events were found (Figure 1).

### 3.2 Analysis of TaAO protein characteristics

To further understand the characteristics of the *TaAO* proteins, protein length, molecular weight, instability index, isoelectric points, average hydrophilicity coefficients, and predicted subcellular localization were analyzed. As shown in Table 1, the protein length of the *TaAOs* ranged from 571 to 641 aa, and molecular weight ranged from 62.5 to 70.7 kDa. Instability index ranged from 30.66 to 39.48, indicating that these *TaAOs* were all stable proteins (instability index < 40). The isoelectric points of these *TaAOs* fell between 5.98 and 6.94, which showed that they were acidic proteins. Their average hydrophilicity coefficients ranged from 0.186 to 0.393, indicating that they were hydrophilic proteins. Subcellular localization prediction *via* the WoLF PSORT software package indicated that *TaAO3-6A*, *TaAO3-6B*, and *TaAO3-6D* were localized to chloroplasts, while *TaAO1-2A*, *TaAO1-2B*, *TaAO3-3D*, *TaAO2-5A*, *TaAO2-5B*, and *TaAO2-5D* were localized to mitochondria. The results of *TaAO3-6D*-GFP fusion protein expression assays showed that *TaAO3-6D* was localized to chloroplasts (Figure 2), which was consistent with the predicted results.

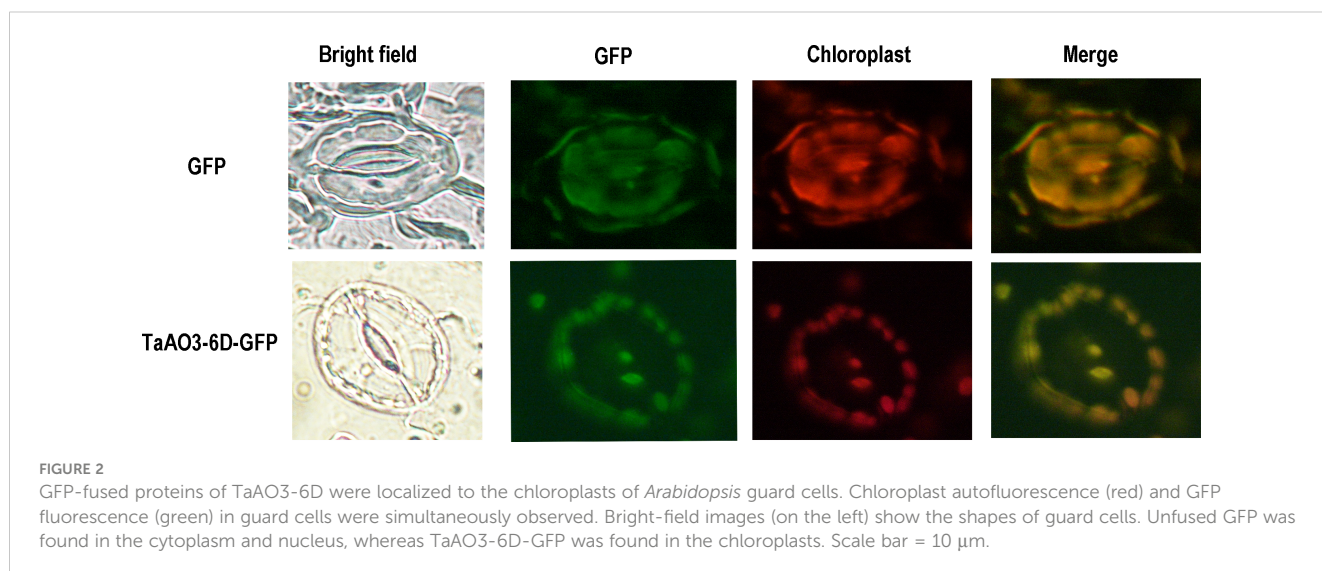
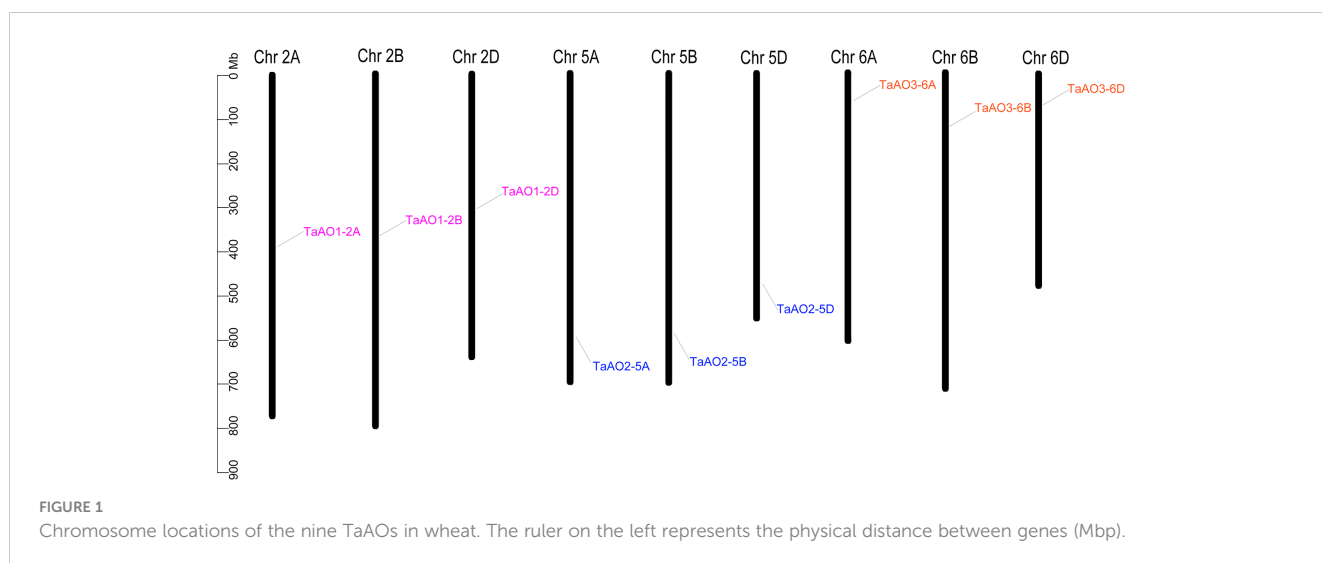
### 3.3 Conserved motifs and gene structures of *TaAOs*

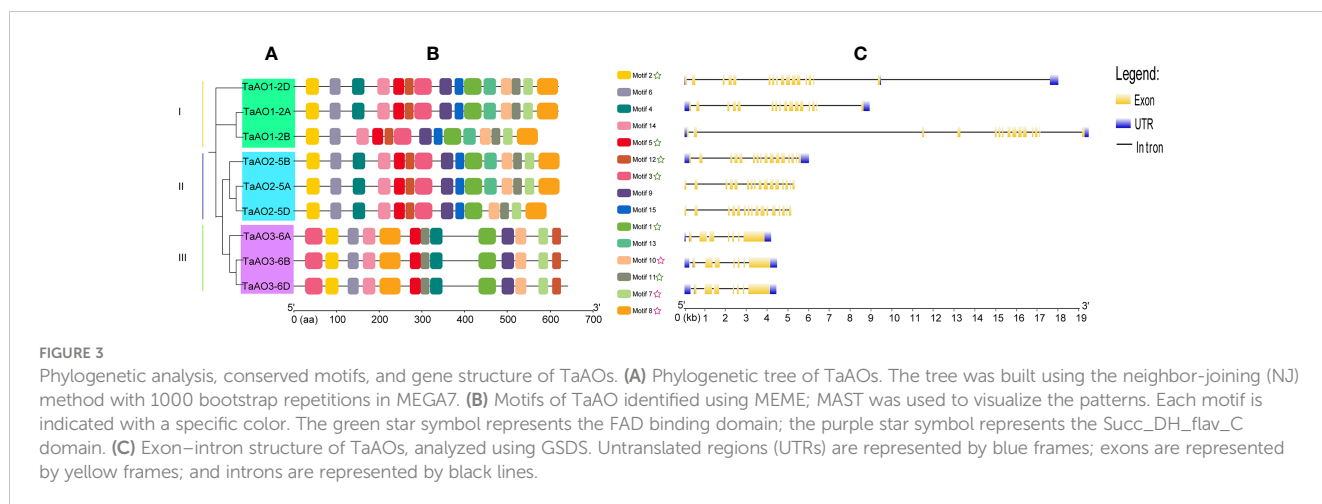
To understand the evolutionary relationships between *TaAOs*, a phylogenetic tree was constructed. As shown in Figure 3A, three *TaAOs* located on chromosome 2 were grouped into Group I, three

TABLE 1 Protein features of AOs in *Triticum aestivum*.

Name	Locus ID	Len	MW	pI	II	Stability	GRAVY	Sub
TaAO1-2A	TraesCS2A03G0615500.1	619	68045.78	6.22	34.07	stable	-0.348	mitochondrion
TaAO1-2B	TraesCS2B03G0694000.1	571	62522.66	6.3	30.66	stable	-0.295	mitochondrion
TaAO1-2D	TraesCS2D03G0589200.1	619	67956.76	6.3	32.97	stable	-0.347	mitochondrion
TaAO2-5A	TraesCS5A03G0972600.1	621	68317.15	6.11	33.17	stable	-0.361	mitochondrion
TaAO2-5B	TraesCS5B03G1021700.1	621	68289.1	6.11	33.31	stable	-0.362	mitochondrion
TaAO2-5D	TraesCS5D03G0925000.1	591	65208.54	5.98	33.98	stable	-0.393	mitochondrion
TaAO3-6A	TraesCS6A03G0227300.1	641	70704.89	6.79	39.48	stable	-0.186	chloroplast
TaAO3-6B	TraesCS6B03G0316000.1	641	70780.01	6.94	38.80	stable	-0.206	chloroplast
TaAO3-6D	TraesCS6D03G0185200.1	641	70639.88	6.94	39.10	stable	-0.194	chloroplast

Len, amino acid length (aa); MW, molecular weight (KDa); pI, isoelectric point; II, instability index; GRAVY, grand average of hydropathy; Sub, subcellular localization.





**FIGURE 3** Phylogenetic analysis, conserved motifs, and gene structure of TaAOs. **(A)** Phylogenetic tree of TaAOs. The tree was built using the neighbor-joining (NJ) method with 1000 bootstrap repetitions in MEGA7. **(B)** Motifs of TaAO identified using MEME; MAST was used to visualize the patterns. Each motif is indicated with a specific color. The green star symbol represents the FAD binding domain; the purple star symbol represents the Succ\_DH\_flav\_C domain. **(C)** Exon–intron structure of TaAOs, analyzed using GSDS. Untranslated regions (UTRs) are represented by blue frames; exons are represented by yellow frames; and introns are represented by black lines.

TaAOs located on chromosome 5 were grouped into Group II, and the three genes located on chromosome 6 were clustered into Group III. The results of a conserved motifs analysis of the TaAOs (Figure 3B; Table S6) showed that all TaAO proteins contained Motifs 1, 2, 3, 5, 7, 8, 10, 11, and 12. Motifs 7, 8, and 10 were contained in the Succ\_DH\_flav\_C domain and Motifs 1, 2, 3, 5, 11, and 12 were contained in the FAD binding domain. The number and order of motifs in TaAOs belonging to Groups I and II were essentially consistent, with the exceptions of TaAO1-2B lacking Motif 4 and TaAO2-5D lacking Motif 13. The number of motifs of Group III members differed from that of members of Groups I and II. TaAOs in Group III only had 13 motifs, from which Motifs 13 and 15 were absent. Furthermore, the order of motifs in Group III also differed from that of the other two groups. Additionally, the results on intron/exon distribution patterns of TaAO genes appeared to indicate that the number of exons was significantly greater in Groups I and II

than in Group III. Generally, TaAOs belonging to Groups I and II contained 16 exons, with the exception of TaAO1-2D, which only contained 15 exons. In contrast, the TaAOs belonging to Group III only contained seven exons (Figure 3C).

### 3.4 Phylogenetic and Ka/Ks analysis of AO genes of *T. aestivum* and its ancestor species

To further evaluate the phylogenetic relationships of TaAOs with other plant AOs, nine AOs from *T. aestivum*, four from *T. urartu*, three from *Ae. Tauschii*, six from *T. dicoccoides*, two from *Oryza sativa*, three from *Zea mays*, and three from *A. thaliana* were used to construct a phylogenetic tree. As shown in Figure 4, the set of all AOs could be divided into three groups, which was consistent

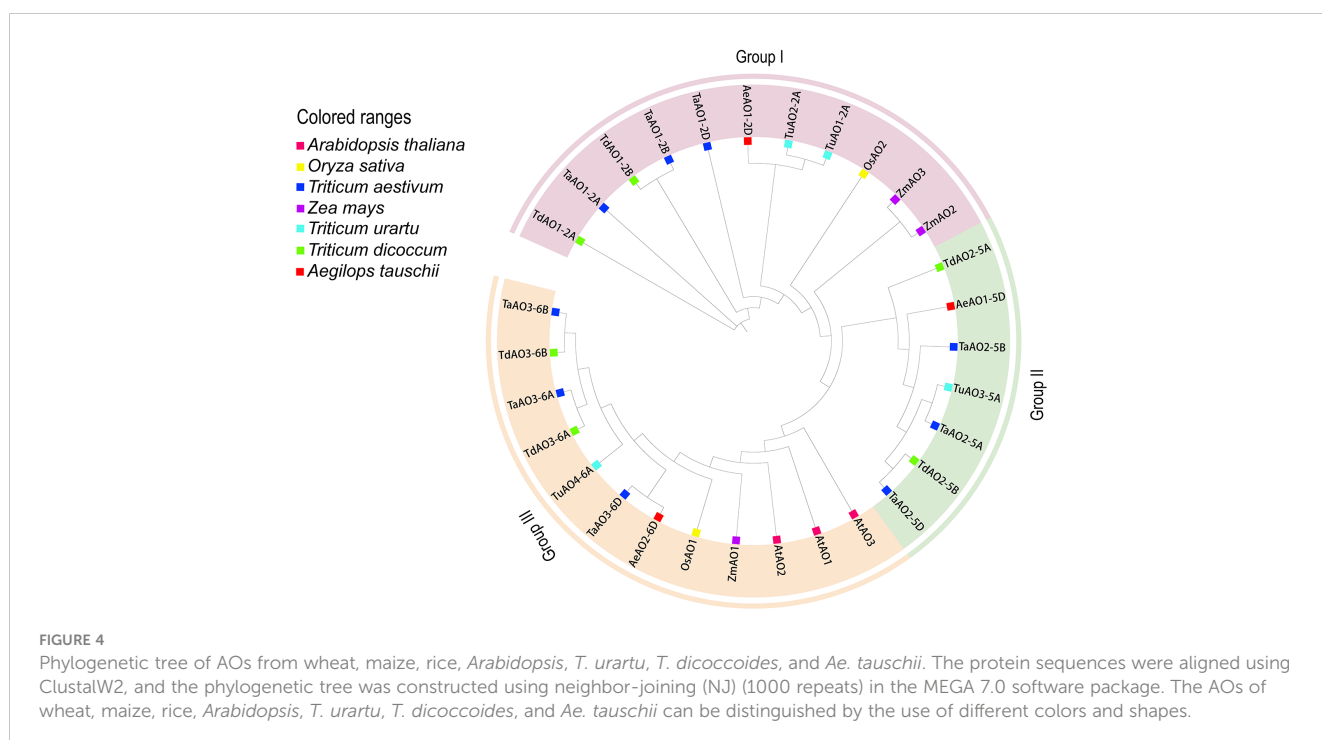


**FIGURE 4** Phylogenetic tree of AOs from wheat, maize, rice, *Arabidopsis*, *T. urartu*, *T. dicoccoides*, and *Ae. tauschii*. The protein sequences were aligned using ClustalW2, and the phylogenetic tree was constructed using neighbor-joining (NJ) (1000 repeats) in the MEGA 7.0 software package. The AOs of wheat, maize, rice, *Arabidopsis*, *T. urartu*, *T. dicoccoides*, and *Ae. tauschii* can be distinguished by the use of different colors and shapes.

with the above-described results on the phylogenetic tree of wheat AOs. TaAOs located on chromosome 2 in different sub-genomes were classified into Group I, TaAOs located on chromosome 5 were in Group II, and TaAOs on chromosome 6 were in Group III (Table S7). It is interesting that all three AtAOs were clustered into Group III, which was found to have the closest relationship with TaAOs on chromosome 6. The AOs of rice and *Zea mays* were classified into Groups I and III, with none falling into Group II. With regard to sub-genome donor species, members were distributed across the three groups. These results indicate that AOs in these species may have evolved under different evolutionary directions, and furthermore, the functions of AOs in different groups may be at variance with one another.

A homology analysis of wheat and three sub-genome donor species was conducted, and the orthologs and paralogs were clustered. Orthologs are defined as genes in different species that are derived from a single gene in the last common ancestor, and paralogs are homologous genes within a single species, resulting from gene duplication (Remm et al., 2001). A total of 53 homologous gene pairs were associated with *T. aestivum* (Figure 5A), of which nine were paralog gene pairs and 44 were ortholog gene pairs were found. Among these 44 ortholog gene

pairs, there were 7, 22, and 15 ortholog genes between *T. aestivum* and each of its ancestor species (*Ae. Tauschii*, *T. dicoccoides*, and *T. Urartu*, respectively). TaAO genes the AOs of *Ae. tauschii*, *T. dicoccoides*, *T. urartu* and *T. aestivum* can be divided into three groups (Figure 5B) were not found in either the domestication-related or the improvement-related sweep regions, and all the Ka/Ks values for AO replication gene pairs were <1 (Figure 5C; Table S8), indicating that TaAO genes were purified and selected, and their functions may be conserved.

### 3.5 Cis-element analysis of TaAO genes

In the process of plant growth and development, not only can cis-regulatory elements regulate the spatio-temporal expression of genes, but they also are involved in responses to phytohormone exposure and abiotic stresses (Davis, 2009). In the present study, 39 kinds of cis-elements were identified in the promoter regions of AO genes in wheat (Figure 6; Table S9). Cis-elements involved in growth and development, including the TATA box and CAAT box, were found in all TaAO promoters. For cis-elements associated with plant hormone responses, the largest set of cis-elements was

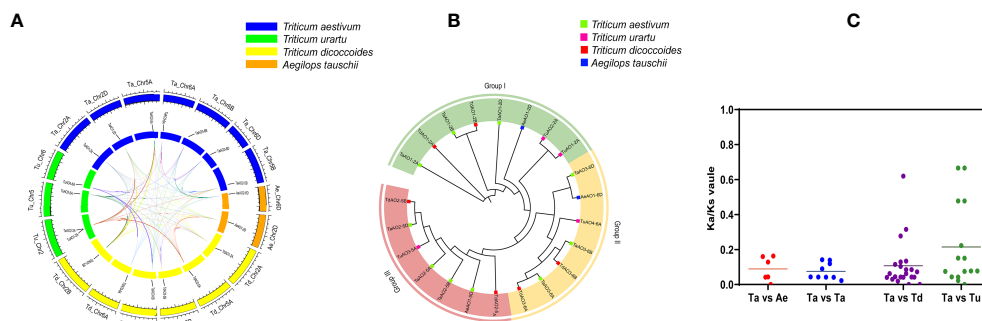


**FIGURE 5** Analysis of (A) synteny and (B) phylogeny for AO genes in *T. aestivum* and its sub-genomic progenitors *T. urartu*, *T. dicoccoides*, and *Ae. Tauschii*. (A) Orange rectangles represent *Ae. tauschii* chromosomes, green rectangles represent *T. urartu* chromosomes, blue rectangles represent *T. aestivum* chromosomes, and yellow rectangles represent *T. dicoccoides* chromosomes. (B) This phylogenetic tree was constructed using 1000 bootstrap repetitions under the neighbor-joining (NJ) method in MEGA7. Blue, red, purple, and green squares represent *Ae. Tauschii*, *T. dicoccoides*, *T. urartu*, and *T. aestivum*, respectively. (C) Ka/Ks values for AO orthologous gene pairs between *T. aestivum*, *T. urartu*, *T. dicoccoides*, and *Ae. Tauschii*.

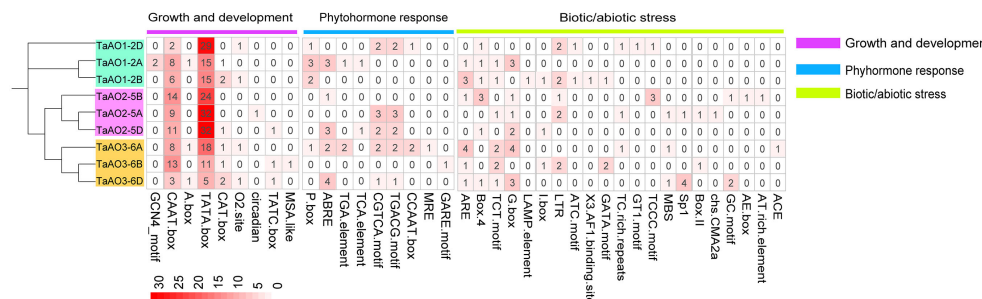


**FIGURE 6** Identification of cis-acting elements of TaAO genes. The color gradient in each grid represents the number of promoter elements of these AO genes.

that of abscisic acid response elements (ABRE), of which 13 were identified. The second largest sets of cis-elements were salicylic acid-associated elements (CGTCA motif and TCA elements); the number of elements identified for each of these was 10. This suggests that the expression of *TaAOs* may be regulated by ABA and SA. The TGACG motif (methyl jasmonate), TGA element (auxin), CGTCA motif, and TCA element (salicylic acid) were identified in most of the *TaAO* gene promoters. In terms of biotic and abiotic stresses, the most abundant cis-element was the G-box, with 14 elements identified, followed by ARE, with 11. This suggests that the expression of *TaAOs* may be regulated by antioxidant/electrophile and photoregulatory factors. In summary, in addition to biotic stress regulation of AO, AO may also be regulated by ABA and SA hormones, as well as antioxidant/electrophile and photoregulatory abiotic stresses.

### 3.6 Molecular interaction networks

A network of the interactions between *TaAOs* and other wheat proteins was built using STRING v11.0. The results showed that all nine *TaAO* proteins interacted with 17 wheat proteins. Among these 17 wheat proteins, seven (Traes\_5BL\_402FB4A3F.1, Traes\_7AL\_C0609756B.1, Traes\_7BL\_8F49CE9D6.2, Traes\_2AS\_4AB51ACE2.1, Traes\_2AS\_BA55E613D.2, Traes\_7AL\_6405AB56F.2, Traes\_4AS\_2DCA42965.1) were unknown proteins, and the remaining ten were Succinate-CoA ligases (Traes\_2DS\_3AC11B9D8.1, Traes\_2AS\_3BA916807.1, Traes\_2BS\_8863D42E7.1), 4Fe-4S ferredoxin-type protein (Traes\_5DL\_885A58CBA.3), lactate/malate dehydrogenase (Traes\_1BL\_A93F9F079.2, Traes\_1DL\_5A31A68D3.2, Traes\_1AL\_2EC98608D.2), malate dehydrogenase

(Traes\_1BL\_BD3E22844.1), succinate dehydrogenase (Traes\_7DL\_91E866851), and transket\_pyr protein (Traes\_2AL\_1E2B26B7F.1) (Figure 7; Table S10). Succinate-CoA ligase (SUCL) can promote the production of ATP during the conversion of malate to succinate in the TCA cycle (Ostergaard, 2008). 4Fe-4S ferredoxin-type protein (4Fe-4S Fed) is involved in various redox processes in organisms, such as DNA repair, RNA and protein modification, and cofactor synthesis (Feng et al., 2021). Lactate/malate dehydrogenases (LDH/MDH) are involved in energy metabolism. Lactate dehydrogenase (LDH) operates at the final stage of aerobic glycolysis. Malate dehydrogenase (MDH) is a key enzyme in the regulation of malate metabolism; it catalyzes the reversible oxidative decarboxylation of malate to produce pyruvate and CO<sub>2</sub>, as well as the reduction of NAD(P)<sup>+</sup> (Zhao et al., 2022). Succinate dehydrogenase (SDH) is the only enzyme that participates in both the tricarboxylic acid or citric acid cycle and the electron transport chain (Gill, 2012). Transket\_pyr protein (TK) plays an important role in carbon metabolism (Liu et al., 2023). These AO-interacting proteins all play important functions in energy metabolism, which explains why AO also plays such an important role in energy metabolism. These results provide clues for further study of the function of *TaAO* genes.

### 3.7 Transcriptome analysis of *TaAOs*

In order to understand the expression patterns of *TaAOs*, wheat transcriptome data taken from different tissues and under exposure to different abiotic and biotic stresses were analyzed. From Figure 8, it is clearly evident that the expression levels of *TaAOs* belonging to Group II were the highest in all selected transcriptomes, which indicates that these three *TaAOs* may play essential roles in plant

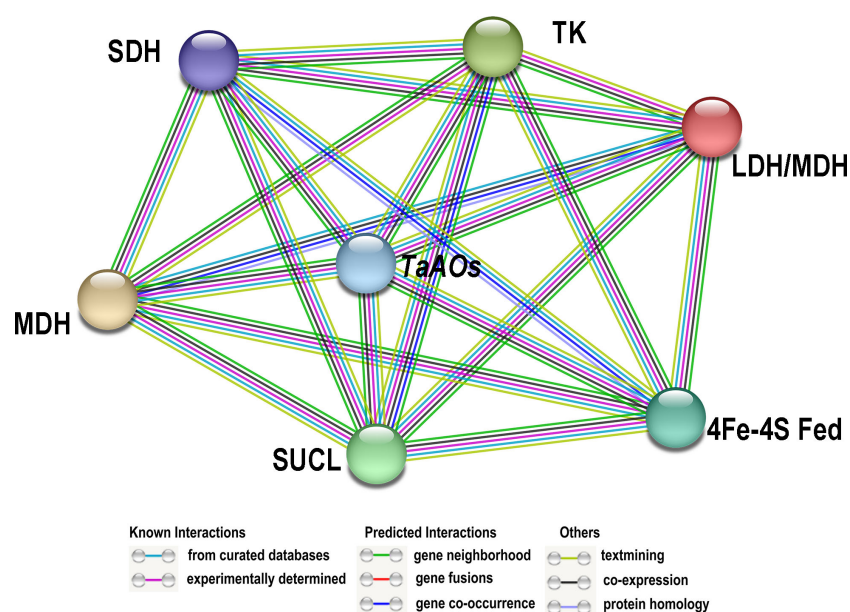
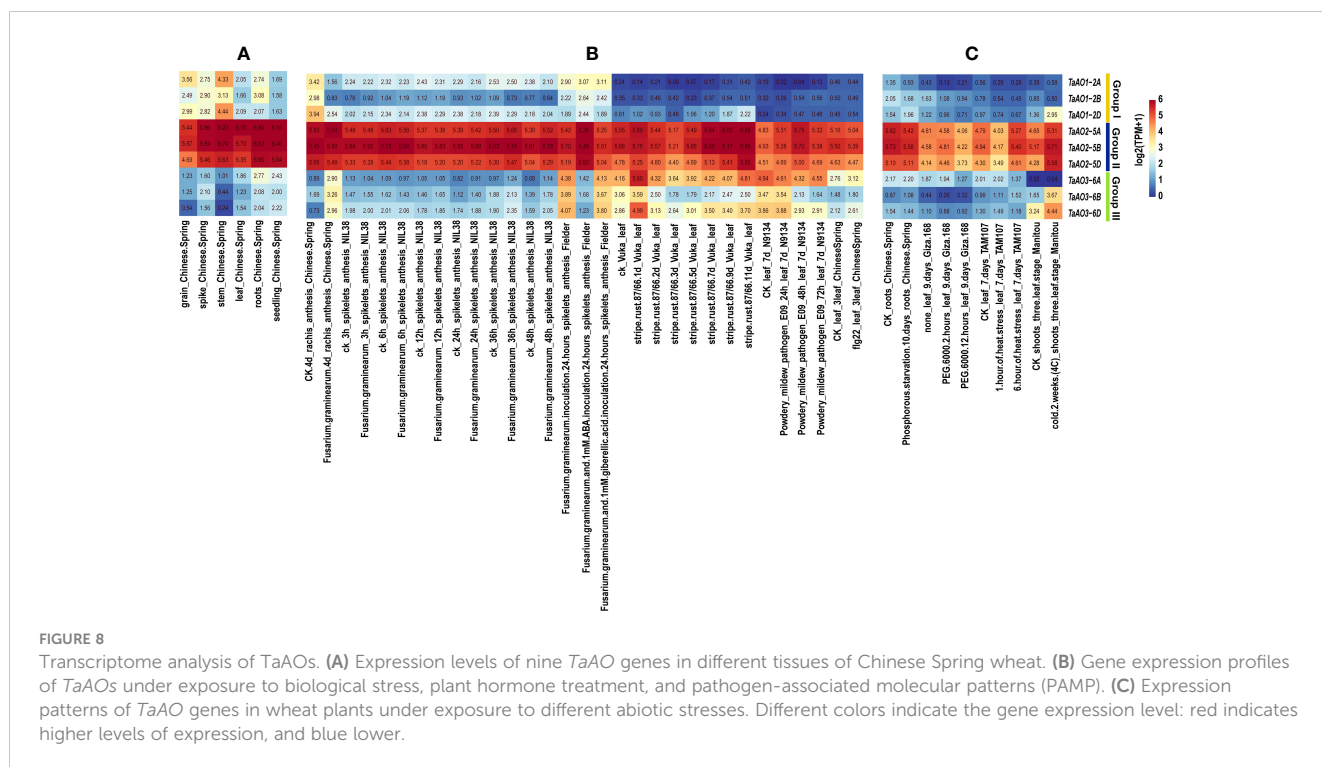


FIGURE 7

Protein-protein interaction (PPI) analysis of *TaAO* proteins. PPI network generated using STRINGV 11.5. Each node denotes a protein, and each edge represents an interaction.



growth and response to various treatments. In terms of the different tissues, TaAOs belonging to Group I were relatively highly expressed in the spike, grain, stem, and root, and TaAOs belonging to Group III were relatively highly expressed in the root and seedling, while TaAOs belonging to Group II were highly expressed in all tissues, with no clear tissue specificity observed (Figure 8A).

As shown in Figure 8B, the transcriptomes of TaAOs under biotic stress were analyzed. In general, the expression of TaAOs changed slightly after infection by stripe rust. With the exceptions of TaAO1-2A and TaAO3-6B, the expression of TaAOs was induced by this form of stress. Interestingly, expression of TaAO1-2D was induced to a large extent at the late stage of infection (9 d and 11 d), while expression of TaAO3-6D was significantly induced at the early stage of infection (1d). These findings suggest that TaAOs might play a role in the response to stripe rust infection, but the patterns of expression were different for different TaAOs. In wheat N9134 from leaf tissue infected by powdery mildew, the expression levels of TaAOs also changed slightly. The expression of TaAO1-2A and TaAOs belonging to Group III was suppressed, while the expression of other TaAOs was induced. The expression of TaAOs was also slightly altered in wheat NIL38 from spikelet tissue infected by *F. graminearum*, but it was greatly altered in *F. graminearum*-infected rachis tissue of Chinese Spring. In rachis tissue infected by *F. graminearum*, the expression of TaAOs belonging to Group I was repressed. The TaAOs with the greatest decrease in expression were TaAO1-2B, the expression levels of which decreased to 11.2% of the levels observed in CK, while the expression of TaAOs belonging to Group III was induced. The TaAOs with the greatest increase in expression were TaAO3-6D, the expression level of which was 10.33 times that observed in CK. These findings indicate that TaAOs may be involved in the pathogenesis of Fusarium head blight, and that

TaAOs belonging to Groups I and III play different roles. Additionally, we found that the expression levels of TaAOs belonging to Group III were much lower in *F. graminearum*-infected wheat spikelet tissue treated with 1 mM ABA than in non-ABA-treated wheat spikelet tissue. This indicates that ABA negatively regulates the expression of TaAOs belonging to Group III in *F. graminearum*-infected wheat spikelets.

As shown in Figure 8C, the transcriptomes of TaAOs under abiotic stress were also analyzed. The results showed that the most significant changes in expression levels of TaAOs were found in wheat in response to cold treatment. The expression of all TaAOs was induced, with the exception of TaAO1-2B, the expression level of which was decreased by half. In contrast, the expression of most TaAOs was repressed during exposure to heat stress and drought stress. These results indicate that most TaAOs may participate in the response to cold and that they play different roles in the responses to heat and drought.

### 3.8 Quantitative real-time PCR analysis

To further understand the potential role of TaAO genes in biotic and abiotic stresses, the patterns of expression of TaAO1-2D, TaAO2-5A, and TaAO3-6D in response to stripe rust infection, ABA, and PEG stress were quantified via qRT-PCR.

After PEG treatment (Figure 9), the expression levels of TaAO1-2D and TaAO2-5A were decreased for 36 hours, but they were subsequently increased at 48 hours after treatment. In contrast, the expression levels of TaAO3-6D were decreased for 48 hours following treatment. In the case of ABA treatment, similar expression patterns were detected in TaAO2-5A and TaAO3-6D, expression of which was suppressed for 48 hours following ABA

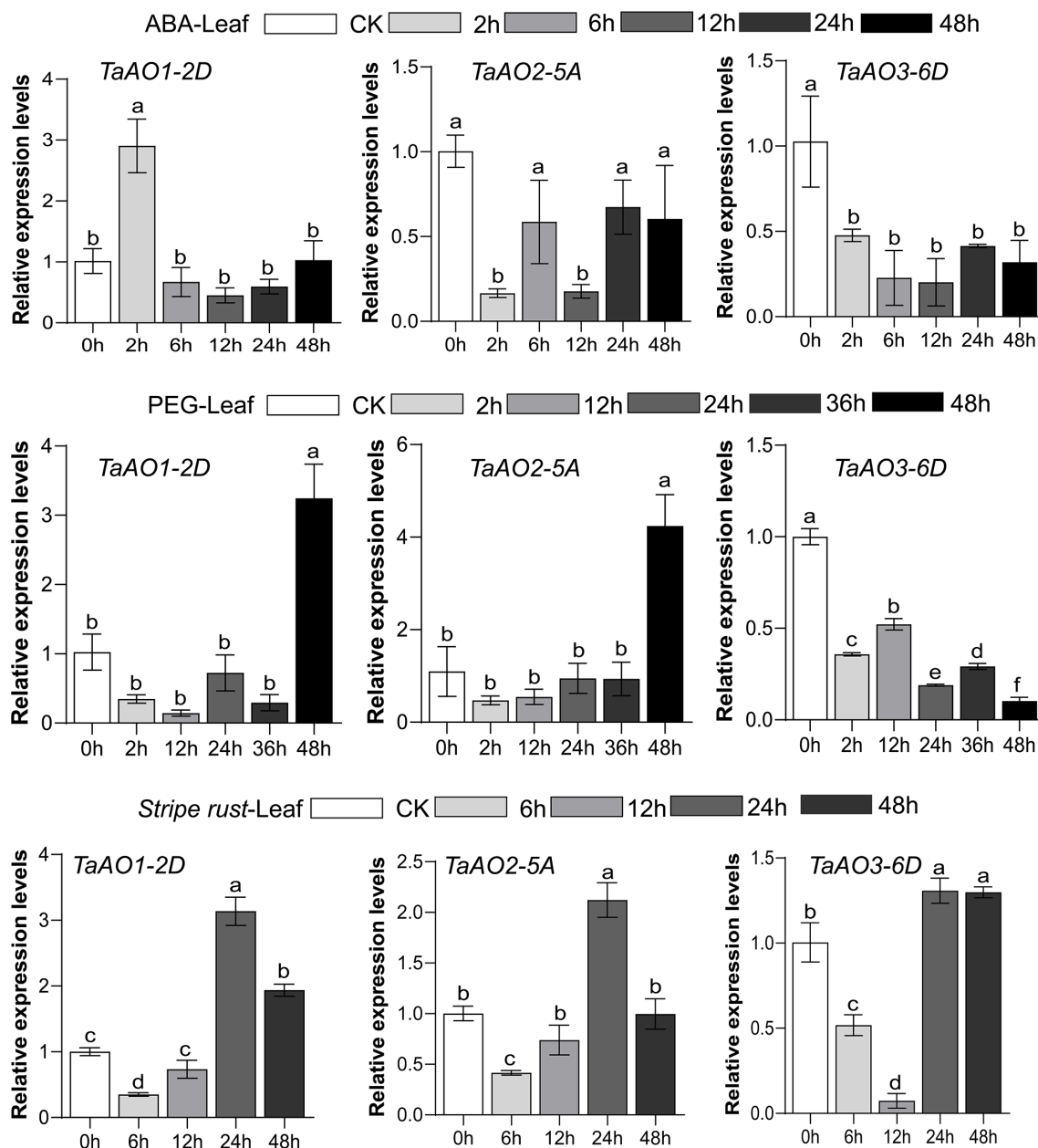


FIGURE 9

Expression levels of three *TaAO* genes in wheat leaves under exposure to abiotic stress (PEG), plant hormone treatment (ABA treatment), and biological stress (stripe rust infection), as indicated by qRT-PCR. The x axis represents time point, and the y axis represents expression level. Data from three independent replicates were analyzed; error bars represent the standard deviation. Lowercase letters (a-f) on the bars indicate significant differences determined via one-way ANOVA ( $P < .05$ ). Plots created using GraphPad Prism 5.

treatment. The pattern of expression of *TaAO1-2D* differed slightly from that of the two aforementioned genes: an increase in the expression level of *TaAO1-2D* was observed 2 hours after ABA treatment.

Finally, in wheat inoculated with stripe rust, the general tendency of expression levels of *TaAO1-2D*, *TaAO2-5A*, and *TaAO3-6D* was to increase after an initial decrease. The lowest level of expression of *TaAO3-6D* was observed at 12 hpi, but the lowest levels for *TaAO1-2D* and *TaAO2-5A* were observed at 6 hpi. Compared with the expression level at 24 hpi, the expression levels

of *TaAO1-2D* and *TaAO2-5A* were decreased at 48 hpi, while the expression level of *TaAO3-6D* at 48 hpi was roughly equal to that at 24 hpi.

## 4 Discussion

NAD<sup>+</sup> is an essential cofactor in energy metabolism and electron transfer. Additionally, several reports suggest that NAD<sup>+</sup> may be involved in plant defense responses (Dutilleul et al., 2003;

Zhang and Mou, 2009; Djebbar et al., 2012; Petriacq et al., 2012). Therefore, as the first enzyme of NAD<sup>+</sup> biosynthesis, AO may influence energy metabolism and plant defense by regulating NAD<sup>+</sup> content. However, this enzyme has previously only been reported in *Arabidopsis* and maize (Macho et al., 2012; Dong, 2019). In this study, we first conducted a systematic analysis of AO-family genes in wheat. The gene architectures, gene duplication events, chromosomal distributions, cis-elements in promoter regions, and expression patterns of AO genes in wheat were then further analyzed.

In this study, nine AOs were identified in wheat. Compared with other plants, the wheat genome encodes many more AOs, which may be due to the heterologous hexaploidy of the wheat genome. In this paper, homology analyses of wheat and three sub-genome donor species were carried out, as a result of which 44 homologous gene pairs were identified, accounting for 90.56% of the wheat orthologous gene pairs. These findings suggest that *TaAOs* are derived from three sub-genome donor species of wheat. Phylogenetic tree analysis of maize, *Arabidopsis*, rice, *T. aestivum*, and its ancestor species (*Ae. tauschii*, *T. dicoccoides*, and *T. urartu*) revealed that Group II only contained *T. aestivum* and its ancestor species. The expression of AOs in Group II was high during growth and development, and under biotic and abiotic stress (Figure 8), indicating that AOs of Group II play an important role in wheat, and that this group has been conserved in the evolution of wheat.

Although AOs are thought to be widely distributed in plants, there has been little investigation of the function of AOs in plants. Up to this point, only two reports on the function of plant AOs have been published (Macho et al., 2012; Dong, 2019). In one of these studies, a differentially expressed *ZmAO* gene involved in energy metabolism was screened from maize CMS-C sterile line C48-2. Compared with the control maintenance line 48-2, *ZmAO* was found to be significantly downregulated in C48-2 during the mononuclear stage of anther development. The *ZmAO* gene may be a positive energy regulator involved in plant growth and development through the NAD<sup>+</sup> synthesis pathway (Dong, 2019). Furthermore, *AtAO2* of *Arabidopsis* is thought to participate in PTI and in resistance to *Pst* DC3000. The expression of AO has been found to be increased in non-virulent DC3000-inoculated *Arabidopsis* (Petriacq et al., 2012). Compared with the wild-type, flg22-triggered ROS bursts are significantly suppressed in *AtAO2* mutants, and *AtAO2* mutants are more susceptible to *Pst* DC3000 (Macho et al., 2012). These two AOs were both found to be members of Group III in the present study and are localized to chloroplasts (Katoh et al., 2006; Dong, 2019). Among the *TaAOs* identified in this study, *TaAO3-6A*, *TaAO3-6B*, and *TaAO3-6D* were also found to be clustered into Group III, and also located in chloroplasts, which suggests that *TaAO3-6A*, *TaAO3-6B*, and *TaAO3-6D* may have similar functions to those of the AOs reported in *Arabidopsis* and maize. Additionally, transcriptome analysis showed that the expression levels of *TaAO3-6A*, *TaAO3-6B*, and *TaAO3-6D* in flg22-treated wheat were increased by 33% to 53% compared with CK. This suggests that *TaAO3-6A*, *TaAO3-6B*, and *TaAO3-6D* may also play a role in PTI in wheat. Moreover, in our study, we found that the expression levels of *TaAOs* belonging to Group III were decreased in wheat treated with powdery mildew

and increased in wheat treated with *F. graminearum* (Figure 8). As we know, the pathogen of wheat powdery mildew is a biotrophic parasite (Spanu et al., 2010), while *F. graminearum* is a hemi-biotrophic pathogen (Ma et al., 2020). These results suggest that *TaAO* may play opposing roles in the pathogenesis of hemi-biotrophic and biotrophic pathogens.

Previous studies have revealed that AO plays important roles in biotic stresses and plant development. In this study, we also found that AO may work in response to abiotic stress. The expression of most *TaAOs* was significantly upregulated under exposure to cold stress and downregulated under combined drought and heat stress. This indicates that AOs play an important role in the adaptation of plants to cold, heat, and drought stress. In summary, this research lays a foundation for further investigation of the function of *TaAOs*.

## 5 Conclusions

In this study, we systematically identified AO genes in wheat genomes. A total of nine *TaAO* genes were identified, which were distributed on three chromosomes of three sub-genomes. *TaAOs* were clustered into three groups. Gene structure and conserved motifs were similar within each group, but differed among the groups. Transcriptome analysis and real-time PCR assay indicated that *TaAOs* belonging to Group II were highly expressed in all tissues. *TaAOs* of Group III were found to be involved in PTI response and in the response to ABA treatment, and were found to play a positive role in wheat resistance to *F. graminearum* infection. Furthermore, *TaAOs* might positively regulate the response to cold treatment. These results provide systematic information on AO in wheat and lay a foundation for further research on the functions of *TaAOs*.

## Data availability statement

The original contributions presented in the study are included in the article/Supplementary Material. Further inquiries can be directed to the corresponding authors.

## Author contributions

WC, ZF, and WW designed the experiments and directed the writing of the manuscript. YF, MT, and JX performed the experiments and wrote the first draft. YF, PL, LW, and WC revised the manuscript. YF and MT contributed to the data analysis. All authors contributed to the article and approved the submitted version.

## Funding

This research was supported by the Open Program of Engineering Research Center of Ecology and Agricultural Use of

Wetland Ministry of Education (KFT202107), the open project program of the State Key Laboratory for Biology of Plant Diseases and Insect Pests (NO. SKLOF202008), and the National Natural Science Foundation of China (31672088).

## Conflict of interest

The authors declare that the research was conducted in the absence of any commercial or financial relationships that could be construed as a potential conflict of interest.

The reviewer XN declared a shared affiliation with the author WW to the handling editor at the time of review.

## References

- Abedi, T., and Mojiri, A. (2020). Cadmium uptake by wheat (*Triticum aestivum* L.): an overview. *Plants (Basel)* 9, 500. doi: 10.3390/plants9040500
- Armenia, I., Balzaretti, R., Pirrone, C., Allegretti, C., D'arrigo, P., Valentino, M., et al. (2017). L-aspartate oxidase magnetic nanoparticles: synthesis, characterization and L-aspartate bioconversion. *Rsc Adv.* 7, 21136–21143. doi: 10.1039/c7ra00384f
- Bacchella, L., Lina, C., Todone, F., Negri, A., Tedeschi, G., Ronchi, S., et al. (1999). Crystallization of L-aspartate oxidase, the first enzyme in the bacterial *de novo* biosynthesis of NAD. *Acta Crystallogr. D Biol. Crystallogr.* 55, 549–551. doi: 10.1107/s0907444998011913
- Bifulco, D., Pollegioni, L., Tessaro, D., Servi, S., and Molla, G. (2013). A thermostable L-aspartate oxidase: a new tool for biotechnological applications. *Appl. Microbiol. Biotechnol.* 97, 7285–7295. doi: 10.1007/s00253-013-4688-1
- Bishop, D. L., and Bugbee, B. G. (1998). Photosynthetic capacity and dry mass partitioning in dwarf and semi-dwarf wheat (*Triticum aestivum* L.). *J. Plant Physiol.* 153, 558–565. doi: 10.1016/s0176-1617(98)80204-6
- Chen, C., Chen, H., Zhang, Y., Thomas, H. R., Frank, M. H., He, Y., et al. (2020). TBtools: an integrative toolkit developed for interactive analyses of big biological data. *Mol. Plant* 13, 1194–1202. doi: 10.1016/j.molp.2020.06.009
- Cheng, H., Liu, J., Wen, J., Nie, X., Xu, L., Chen, N., et al. (2019). Frequent intra- and inter-species introgression shapes the landscape of genetic variation in bread wheat. *Genome Biol.* 20, 136. doi: 10.1186/s13059-019-1744-x
- Chou, K. C., and Shen, H. B. (2010). Plant-mPLoc: a top-down strategy to augment the power for predicting plant protein subcellular localization. *PLoS One* 5, e11335. doi: 10.1371/journal.pone.0011335
- Chow, C., Hegde, S., and Blanchard, J. S. (2017). Mechanistic characterization of *Escherichia coli* L-aspartate oxidase from kinetic isotope effects. *Biochemistry* 56, 4044–4052. doi: 10.1021/acs.biochem.7b00307
- Davis, S. J. (2009). Integrating hormones into the floral-transition pathway of *Arabidopsis thaliana*. *Plant Cell Environ.* 32, 1201–1210. doi: 10.1111/j.1365-3040.2009.01968.x
- Djebbar, R., Rzigui, T., Petriacq, P., Mauve, C., Priault, P., Fresneau, C., et al. (2012). Respiratory complex I deficiency induces drought tolerance by impacting leaf stomatal and hydraulic conductances. *Planta* 235, 603–614. doi: 10.1007/s00425-011-1524-7
- Dong, B. (2019). The functional analysis of differentially expressed genes ZmA1 and ZmA0 in maize CMS-c CNKI. *CNKI* 7, 7–10. doi: 10.27345/d.cnki.gsnyu.2019.001308
- Dutilleul, C., Garmier, M., Noctor, G., Mathieu, C., Chetrit, P., Foyer, C. H., et al. (2003). Leaf mitochondria modulate whole cell redox homeostasis, set antioxidant capacity, and determine stress resistance through altered signaling and diurnal regulation. *Plant Cell* 15, 1212–1226. doi: 10.1105/tpc.009464
- Fang, Z. W., He, Y. Q., Liu, Y. K., Jiang, W. Q., Song, J. H., Wang, S. P., Yin, J. L., et al. (2020). Bioinformatic identification and analyses of the non-specific lipid transfer proteins in wheat. *J. Integr. Agric.* 19, 1170–1185. doi: 10.1016/S2095-3119(19)62776-0
- Feng, J. Q., Shaik, S., and Wang, B. J. (2021). Spin-regulated electron transfer and exchange-enhanced reactivity in Fe4S4-mediated redox reaction of the Dph2 enzyme during the biosynthesis of diphthamide. *Angewandte Chemie-International Edition* 60, 20430–20436. doi: 10.1002/anie.202107008
- Gakiere, B., Hao, J. F., De Bont, L., Petriacq, P., Nunes-Nesi, A., and Fernie, A. R. (2018). NAD(+) biosynthesis and signaling in plants. *Crit. Rev. Plant Sci.* 37, 259–307. doi: 10.1080/07352689.2018.1505591
- Gasteiger, E., Gattiker, A., Hoogland, C., Ivanyi, I., Appel, R. D., and Bairoch, A. (2003). ExPASy: the proteomics server for in-depth protein knowledge and analysis. *Nucleic Acids Res.* 31, 3784–3788. doi: 10.1093/nar/gkg563
- Gill, A. J. (2012). Succinate dehydrogenase (SDH) and mitochondrial driven neoplasia. *Pathology* 44, 285–292. doi: 10.1097/PAT.0b013e3283539932
- Guo, G., Lei, M., Wang, Y., Song, B., and Yang, J. (2018). Accumulation of as, cd, and Pb in sixteen wheat cultivars grown in contaminated soils and associated health risk assessment. *Int. J. Environ. Res. Public Health* 15, 2601. doi: 10.3390/ijerph15112601
- Hao, J., Petriacq, P., De Bont, L., Hodges, M., and Gakiere, B. (2018). Characterization of L-aspartate oxidase from *Arabidopsis thaliana*. *Plant Sci.* 271, 133–142. doi: 10.1016/j.plantsci.2018.03.016
- Katoh, A., Uenohara, K., Akita, M., and Hashimoto, T. (2006). Early steps in the biosynthesis of NAD in *Arabidopsis* start with aspartate and occur in the plastid. *Plant Physiol.* 141, 851–857. doi: 10.1104/pp.106.081091
- Kumar, S., Stecher, G., Li, M., Knyaz, C., and Tamura, K. (2018). MEGA X: molecular evolutionary genetics analysis across computing platforms. *Mol. Biol. Evol.* 35, 1547–1549. doi: 10.1093/molbev/msy096
- Leese, C., Fotheringham, I., Escalettes, F., Speight, R., and Grogan, G. (2013). Cloning, expression, characterisation and mutational analysis of L-aspartate oxidase from *Pseudomonas putida*. *J. Mol. Catalysis B-Enzymatic* 85–86, 17–22. doi: 10.1016/j.molcatb.2012.07.008
- Letunic, I., and Bork, P. (2018). 20 years of the SMART protein domain annotation resource. *Nucleic Acids Res.* 46, D493–D496. doi: 10.1093/nar/gkx922
- Letunic, I., and Bork, P. (2021). Interactive tree of life (iTOL) v5: an online tool for phylogenetic tree display and annotation. *Nucleic Acids Res.* 49, W293–W296. doi: 10.1093/nar/gkab301
- Liu, G., Liu, Q., Han, Z., Wang, P., and Li, Y. (2023). Comparative proteomics analysis of adult *haemaphysalis contortus* isolates from *Ovis ammon*. *Front. Cell Infect. Microbiol.* 13. doi: 10.3389/fcimb.2023.1087210
- Ma, Z., Xie, Q., Li, G., Jia, H., Zhou, J., Kong, Z., et al. (2020). Germplasm, genetics and genomics for better control of disastrous wheat fusarium head blight. *Theor. Appl. Genet.* 133, 1541–1568. doi: 10.1007/s00122-019-03525-8
- Macho, A. P., Boutrot, F., Rathjen, J. P., and Zipfel, C. (2012). Aspartate oxidase plays an important role in *Arabidopsis* stomatal immunity. *Plant Physiol.* 159, 1845–1856. doi: 10.1104/pp.112.199810
- Marinoni, I., Nonnis, S., Monteferrante, C., Heathcote, P., Hartig, E., Bottger, L. H., et al. (2008). Characterization of L-aspartate oxidase and quinolinate synthase from *Bacillus subtilis*. *FEBS J.* 275, 5090–5107. doi: 10.1111/j.1742-4658.2008.06641.x
- Mattevi, A., Tedeschi, G., Bacchella, L., Coda, A., Negri, A., and Ronchi, S. (1999). Structure of L-aspartate oxidase: implications for the succinate dehydrogenase/fumarate reductase oxidoreductase family. *Structure* 7, 745–756. doi: 10.1016/s0969-2126(99)80099-9
- Mortarino, M., Negri, A., Tedeschi, G., Simonic, T., Duga, S., Gassen, H. G., et al. (1996). L-aspartate oxidase from *Escherichia coli*. I. characterization of coenzyme binding and product inhibition. *Eur. J. Biochem.* 239, 418–426. doi: 10.1111/j.1432-1033.1996.0418u.x
- Nasu, S., Wicks, F. D., and Gholson, R. K. (1982). L-aspartate oxidase, a newly discovered enzyme of *Escherichia coli*, is the b protein of quinolinate synthetase. *J. Biol. Chem.* 257, 626–632. doi: 10.1016/S0021-9258(19)68239-6

## Publisher's note

All claims expressed in this article are solely those of the authors and do not necessarily represent those of their affiliated organizations, or those of the publisher, the editors and the reviewers. Any product that may be evaluated in this article, or claim that may be made by its manufacturer, is not guaranteed or endorsed by the publisher.

## Supplementary material

The Supplementary Material for this article can be found online at: <https://www.frontiersin.org/articles/10.3389/fpls.2023.1210632/full#supplementary-material>

- Ostergaard, E. (2008). Disorders caused by deficiency of succinate-CoA ligase. *J. Inherit. Metab. Dis.* 31, 226–229. doi: 10.1007/s10545-008-0828-7
- Panchy, N., Lehti-Shiu, M., and Shiu, S. H. (2016). Evolution of gene duplication in plants. *Plant Physiol.* 171, 2294–2316. doi: 10.1104/pp.16.00523
- Petriacq, P., De Bont, L., Hager, J., Didierlaurent, L., Mauve, C., Guerard, F., et al. (2012). Inducible NAD overproduction in arabidopsis alters metabolic pools and gene expression correlated with increased salicylate content and resistance to pst-AvrRpm1. *Plant J.* 70, 650–665. doi: 10.1111/j.1365-313X.2012.04920.x
- Prunier, A. L., Schuch, R., Fernandez, R. E., Mumy, K. L., Kohler, H., McCormick, B. A., et al. (2007). nadA and nadB of shigella flexneri 5a are antivirulence loci responsible for the synthesis of quinolinate, a small molecule inhibitor of shigella pathogenicity. *Microbiol. (Reading)* 153, 2363–2372. doi: 10.1099/mic.0.2007/006916-0
- Remm, M., Storm, C. E., and Sonnhammer, E. L. (2001). Automatic clustering of orthologs and in-paralogs from pairwise species comparisons. *J. Mol. Biol.* 314, 1041–1052. doi: 10.1006/jmbi.2000.5197
- Ren, Y., Liu, L. S., He, Z. H., Wu, L., Bai, B., and Xia, X. C. (2015). QTL mapping of adult-plant resistance to stripe rust in a "Lumai 21xJingshuang 16" wheat population. *Plant Breed.* 134, 501–507. doi: 10.1111/pbr.12290
- Rombauts, S., Dehais, P., Van Montagu, M., and Rouze, P. (1999). PlantCARE, a plant cis-acting regulatory element database. *Nucleic Acids Res.* 27, 295–296. doi: 10.1093/nar/27.1.295
- Sakuraba, H., Satomura, T., Kawakami, R., Yamamoto, S., Kawarabayasi, Y., Kikuchi, H., et al. (2002). L-aspartate oxidase is present in the anaerobic hyperthermophilic archaeon pyrococcus horikoshii OT-3: characteristics and role in the *de novo* biosynthesis of nicotinamide adenine dinucleotide proposed by genome sequencing. *Extremophiles* 6, 275–281. doi: 10.1007/s00792-001-0254-3
- Sakuraba, H., Yoneda, K., Asai, I., Tsuge, H., Katunuma, N., and Ohshima, T. (2008). Structure of l-aspartate oxidase from the hyperthermophilic archaeon sulfobolus tokodaii. *Biochim. Biophys. Acta* 1784, 563–571. doi: 10.1016/j.bbapap.2007.12.012
- Santra, D. K., Chen, X. M., Santra, M., Campbell, K. G., and Kidwell, K. K. (2008). Identification and mapping QTL for high-temperature adult-plant resistance to stripe rust in winter wheat (*Triticum aestivum* L.) cultivar 'Stephens'. *Theor. Appl. Genet.* 117, 793–802. doi: 10.1007/s00122-008-0820-5
- Sobolewska, M., Wenda-Piesik, A., Jaroszewska, A., and Stankowski, S. (2020). Effect of habitat and foliar fertilization with K, zn and Mn on winter wheat grain and baking qualities. *Agronomy-Basel* 10, 276. doi: 10.3390/agronomy10020276
- Spanu, P. D., Abbott, J. C., Amselem, J., Burgis, T. A., Soanes, D. M., Stuber, K., et al. (2010). Genome expansion and gene loss in powdery mildew fungi reveal tradeoffs in extreme parasitism. *Science* 330, 1543–1546. doi: 10.1126/science.1194573
- Tedeschi, G., Negri, A., Mortarino, M., Cecilian, F., Simonic, T., Faotto, L., et al. (1996). L-aspartate oxidase from escherichia coli. II. interaction with C4 dicarboxylic acids and identification of a novel l-aspartate: fumarate oxidoreductase activity. *Eur. J. Biochem.* 239, 427–433. doi: 10.1111/j.1432-1033.1996.0427u.x
- Tedeschi, G., Nonnis, S., Strumbo, B., Cruciani, G., Carosati, E., and Negri, A. (2010). On the catalytic role of the active site residue E121 of e. coli l-aspartate oxidase. *Biochimie* 92, 1335–1342. doi: 10.1016/j.biochi.2010.06.015
- Thompson, J. D., Higgins, D. G., and Gibson, T. J. (1994). CLUSTAL W: improving the sensitivity of progressive multiple sequence alignment through sequence weighting, position-specific gap penalties and weight matrix choice. *Nucleic Acids Res.* 22, 4673–4680. doi: 10.1093/nar/22.22.4673
- Trapnell, C., Roberts, A., Goff, L., Pertea, G., Kim, D., Kelley, D. R., et al. (2012). Differential gene and transcript expression analysis of RNA-seq experiments with TopHat and cufflinks. *Nat. Protoc.* 7, 562–578. doi: 10.1038/nprot.2012.016
- Zhang, X., and Mou, Z. (2009). Extracellular pyridine nucleotides induce PR gene expression and disease resistance in arabidopsis. *Plant J.* 57, 302–312. doi: 10.1111/j.1365-313X.2008.03687.x
- Zhao, M. J., Yao, P. B., Mao, Y. X., Wu, J. J., Wang, W. H., Geng, C. H., et al. (2022). Malic enzyme 2 maintains protein stability of mutant p53 through 2-hydroxyglutarate. *Nat. Metab.* 4, 225–22+. doi: 10.1038/s42255-022-00532-w